Electronic Supplementary Information

Crystal-surface-induced simultaneous synthesis and hierarchical morphogenesis of conductive polymers

Kento Kuwabara, Yuya Oaki,* Ryo Muramatsu, Hiroaki Imai*

Department of Applied Chemistry, Faculty of Science and Technology, Keio University, 3-14-1 Hiyoshi, Kohoku-ku, Yokohama 223-8522, Japan

*E-mail: oakiyuya@applc.keio.ac.jp (Y. O.), hiroaki@applc.keio.ac.jp (H. I.)

Contents

Experimental Procedure

Materials. Monomers of aniline (Ani, Wako 98 %), pyrrole (Py, TCI 99%), thiophene (Tp, TCI 98 %), 3,4-ethylenedioxythiophene (EDOT, TCI 98 %), and 3-hexylthiophene (3HT, TCI 98 %) were used as purchased without further purification. Inorganic crystals of iron chloride ($FeCl_3$, Wako 95 %), copper bromide ($CuBr_2$, Wako 99 %), copper nitrate trihydrate ($Cu(NO_3)_2 \cdot 3H_2O$, Wako 99 %), copper chloride dihydrate ($CuCl_2 \cdot 2H_2O$, Kanto 98.5 %), silver nitrate ($AgNO_3$, Kanto 99.7 %), copper acetate monohydrate ($Cu(CH_3COO)_2 \cdot H_2O$, Kanto 98.5 %), and copper sulfate pentahydrate ($CuSO_4 \cdot 5H_2O$, Kanto 99.0 %) were used as purchased without further purification.

Polymerization of the heteroaromatic monomers. The typical experimental setup was illustrated in Fig. 1a. Two small polypropylene vessels, typically 6 cm^3, each containing 500 mg of the oxidant crystal and 0.3 cm^3 of the monomer were put in a large size, typically 250 cm^3, of polypropylene vessel. The sealed outer vessel was maintained at 60 °C for 15 min to 48 h. After the reaction, the oxidant crystals coated with the polymerized materials were washed with an excess amount of 1 mol dm^{-3} hydrochloric acid (HCl) and ethanol. The resultant polymer materials were dried at 60 °C.

Synthesis of the porous PPy by using freeze-dried $CuSO_4 \cdot 5H_2O$ crystals. A glass vessel containing 5 cm^3 of 20 mg cm^{-3} $CuSO_4 \cdot 5H_2O$ aqueous solution was immersed in a liquid nitrogen. After completely frozen, the glass vessel was attached to the equipment of freeze dry (Tokyo Rikakikai, FDU-1200). The frozen solution was dried at room temperature under vacuum conditions. The polymerization was performed on the freeze-dried $CuSO_4 \cdot 5H_2O$ crystals by the same method as mentioned above. After the polymerization, the residual inorganic species were dissolved by an excess amount of 1 mol dm^{-3} HCl and ethanol. Then, the resultant PPy architecture was freeze-dried.

Characterization. The morphologies of the resultant materials were observed by optical

microscopy (Keyence VHX-1000) and field-emission scanning electron microscopy (FESEM, FEI Sirion, Hitachi S-4700, and JEOL JSM7600F) operated at 5.0 kV. The resultant polymers were characterized by Fourier-transform infrared (FT-IR) absorption spectroscopy (JASCO, FT/IR-4200). The samples were prepared by mixing with potassium bromide (KBr). The residual metal-related components were analyzed by energy-dispersive X-ray spectroscopy (EDX, Bruker Quantax) on the FE-SEM observation and thermogravimetry (TG, SII TG-DTA7000). The UV-Vis absorption spectroscopy was measured by the dispersion liquid of the resultant PANI (JASCO, V-670). The changes of the crystal structures after reaction were analyzed by X-ray diffraction (XRD, Rigaku Mini Flex II) with Cu-Kα radiation.

Electrochemical properties. The electrochemical measurement was performed by using a three electrode setup in a twin-beaker cell. The working electrode was prepared by mixing of 80 wt-% PPy samples, 10 wt-% acetylene black carbon, and 10 wt-% poly(vinylidene fluoride) (PVDF) binder. The slurry of these materials in N-methyl-2-pyrrolidone was dropped on a titanium mesh as a current collector. The resultant electrode was dried for more than 12 h at room temperature under vacuum conditions. A platinum-coated silicon plate and Ag/AgCl electrode were used as the counter and reference electrodes, respectively. Chronopotentiometry measurement was performed in 1 mol dm^{-3} potassium chloride (KCl) aqueous solution by using charge-discharge measurement system (Hokuto Denko, HJ1001SD8) in the potential range from –0.2 V to 0.6 V vs. Ag/AgCl at the different current density. The commercial PPy fibers (Aldrich) was used as purchased without purification.

Structure analyses of the resultant PAni

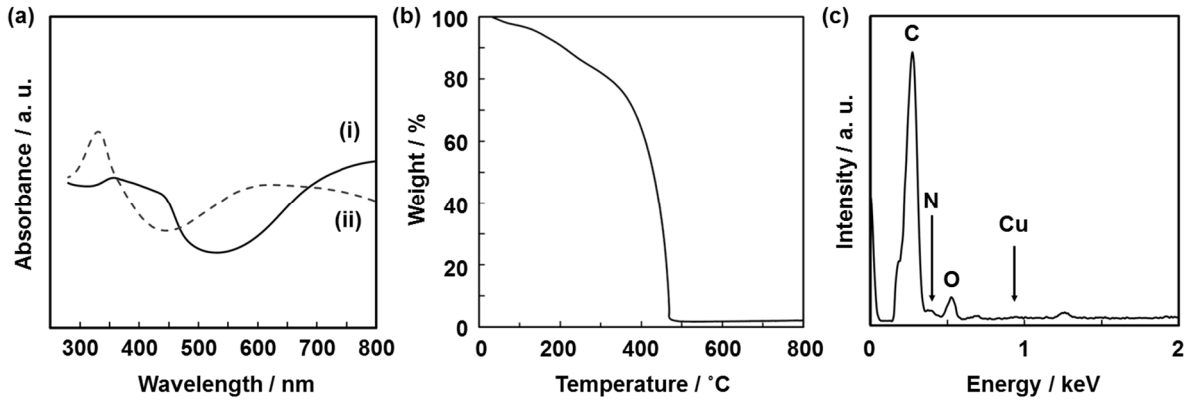

Fig. S1. UV-Vis spectra (a), TG curve (b), and EDX spectrum (c) of the resultant PAni on the $Cu(NO_3)_2 \cdot 3H_2O$ crystals. The UV-Vis spectra were obtained from the dispersion liquid of the resultant PAni in 1 mol dm^{-3} HCl solution (spectrum (i)) and ca. 30 vol.% NH_3 aqueous solution (spectrum (ii)).

The PAni dispersion liquid was obtained after the dissolution of $Cu(NO_3)_2 \cdot 3H_2O$ crystals in 1 mol dm^{-3} HCl. The UV-Vis spectrum shows the broadened absorption bands from 350 nm to 420 nm (spectrum (i) in Fig. S1a). The absorption corresponds to the electron transitions of π-π^* and polaron-π^* in the doped state of PAni.[18] After the centrifugation, the collected PAni precipitate was dispersed in an aqueous solution of ca. 30 vol % NH_3 to prepare the dedoped PAni. The UV-Vis spectrum shows the broadened absorption bands centered at 330 nm to 600 nm (spectrum (ii) in Fig. S1a). The absorption corresponds to the electron transitions of π-π^* and charge-transfer excitation in the dedoped state of PAni. The TG and EDX analyses were performed on the PAni samples after the dissolution of $Cu(NO_3)_2 \cdot 3H_2O$ by HCl. The weight loss indicates the presence of the residue about 2.9 wt % in the resultant PAni (Fig. S1b). The EDX analysis suggests the inclusion of copper related compounds and chloride anions as the dopant (Fig. S1c). These results suggest that a trace amount of the residual copper-related compounds were contained in the resultant PAni architectures.

XRD patterns of the oxidant crystals after the polymerization

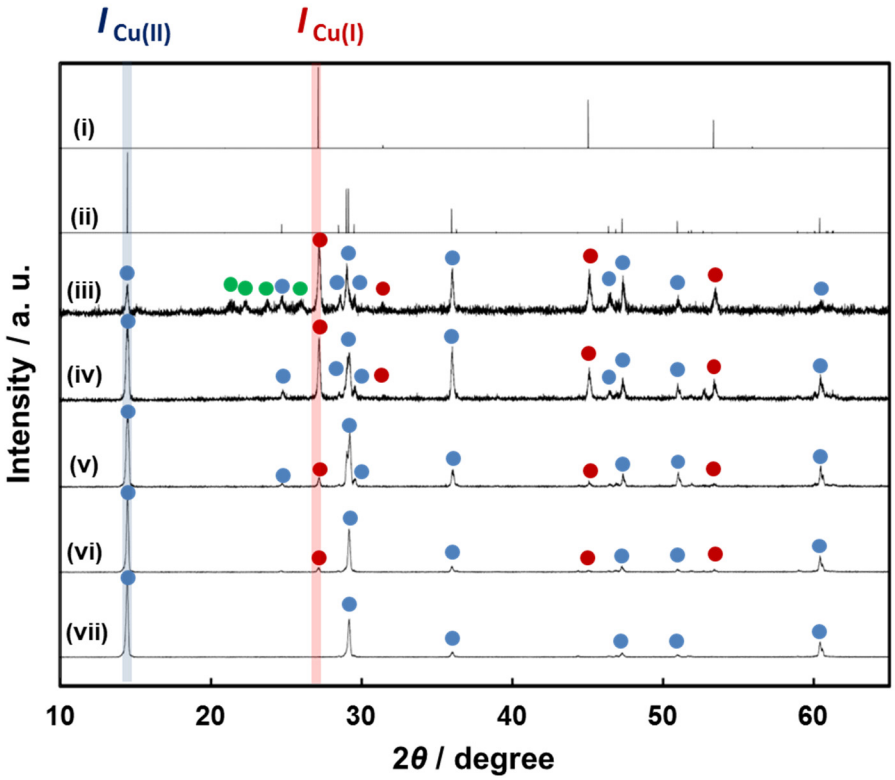

Fig. S2. XRD patterns of the $CuBr_2$ crystals after the polymerization of Ani for 64 h (iii), Py for 48 h (iv), EDOT for 7 days (v), Tp for 7 days (vi), and 3HT for 7 days (vii). The bars in the (i) and (ii) indicate the peak positions of γ-CuBr crystal (red circles, ICDD: 00-006-0292) and $CuBr_2$ crystal (blue circles, ICDD: 00-045-1063). The unknown peaks are represented by the green circles.

As the polymerization proceeded with Ani, Py, EDOT, and Tp monomers, the crystals of $CuBr_2$ turned to those of γ-CuBr with reduction of divalent copper ions. The corresponding polymers were obtained on the crystal surface (Table 1 and Fig. S3). The strongest peaks of γ-CuBr and $CuBr_2$ were marked by the red ($I_{Cu(II)}$) and blue ribbons ($I_{Cu(I)}$), respectively. The peak intensity ratio $R=I_{Cu(I)}/I_{Cu(II)}$ represents the polymerization rates. The R values are calculated to be 3.16 for Ani, 6.85×10^{-1} for Py, 1.11×10^{-1} for EDOT, 5.94×10^{-2} for Th, and 0 for 3HT. The reduction behavior was not observed on the $CuBr_2$ crystal with 3HT. These results support that the oxidative polymerization proceeds on the surface with the reduction of the oxidant crystals. The reaction rates depend on the combinations of the monomers and oxidant crystals.

FT-IR spectra of the other conductive polymers

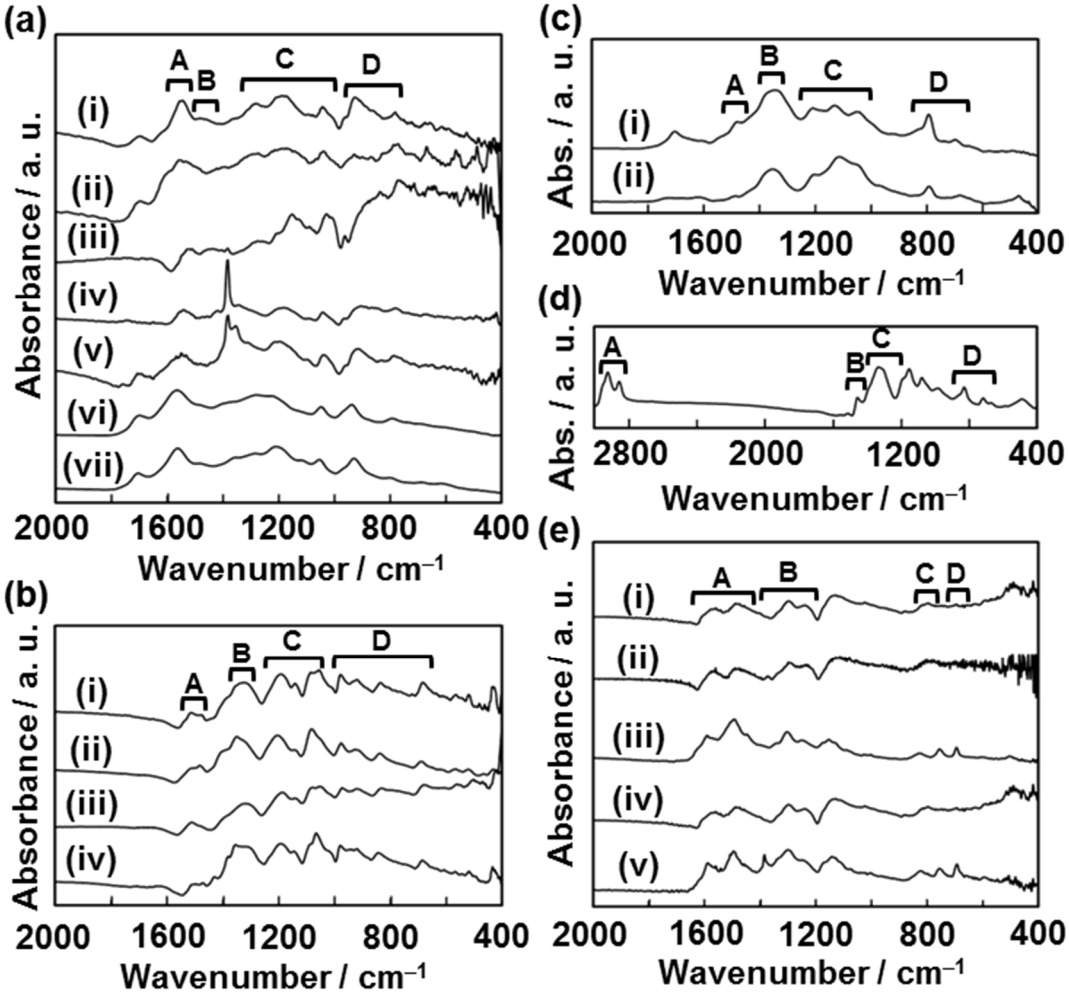

Fig. S3. FT-IR spectra of the conductive polymers synthesized by the combinations as listed in Table 1. (a) PPy formed on the surface of $FeCl_3$ for 168 h (i), $CuBr_2$ for 168 h (ii), $CuCl_2 \cdot 2H_2O$ for 90 h (iii), $Cu(NO_3)_2 \cdot 3H_2O$ for 40 h (iv), $AgNO_3$ for 504 h (v), $Cu(CH_3COO)_2 \cdot H_2O$ for 48 h (vi), and $CuSO_4 \cdot 5H_2O$ for 40 h (vii). (b) PEDOT formed on the surface of $FeCl_3$ for 168 h (i), $CuBr_2$ (ii) for 168 h, $CuCl_2 \cdot 2H_2O$ for 48 h (iii), and $AgNO_3$ for 504 h (iv). (c) PTp formed on the surface of $FeCl_3$ for 168 h (i) and $CuBr_2$ for 168 h (ii). (d) P3HT formed on the surface of $FeCl_3$ for 48 h. (e) PAni formed on the surface of $FeCl_3$ for 66 h (i), $CuBr_2$ for 64 h (ii), $CuCl_2 \cdot 2H_2O$ for 264 h (iii), $Cu(NO_3)_2 \cdot 3H_2O$ for 40 h (iv), and $AgNO_3$ for 16 h (v).

The assignments of the absorption bands were referred to the previous reports of PPy,[S1] PEDOT,[S2] PTp,[S1,S3] P3HT,[S4] and PAni,[19] In Fig. S3a, the absorption bands of PPy were assigned to the following vibrations: C=C stretching (A), C–N stretching (B), C–H in-plane bending (C), and

C–H out-of-plane bending (D). In Fig. S3b, the absorption bands of PEDOT were assigned to the following vibrations: C=C stretching (A), C-C stretching (B), C–O–C stretching (C), and C–S stretching (D). In Fig. S3c, the absorption bands of PTp were assigned to the following vibrations: C=C stretching (A), C–C stretching (B), C–H in-plane bending (C), and C-S stretching (D). In Fig. S3d, the absorption bands of P3HT were assigned to the following vibrations: C–H stretching (A), C=C stretching (B), C–H in-plane bending (C), and C–H out-of-plane bending (D). In Fig. S3e, the absorption bands of PAni were assigned to the following vibrations: C=C stretching (A), C–N stretching (B), C-H out-of-plane bending (C), and out-of-plane bending (D). These results support the formation of the conductive polymers in the combinations of the monomers and oxidant crystals in Table 1.

Additional References

S1. K. Majid, R. Tabassum, A. F. Shah, S. Ahmad and M. L. Singla, *J. Mater. Sci. Mater. Electron*, 2009, **20**, 958.

S2. C. Jiang, G. Chen, and X. Wang, *Synth. Met.*, 2012, **162**, 1968.

S3. A. Gök, M. Omastová and A. G. Yavuz, *Synth. Met*., 2007, **157**, 23.

S4. H. Wei, L. Scudiero and H. Eilers, *Appl. Surf. Sci.*, 2009, **255**, 8593.

FESEM images of the other conductive polymers

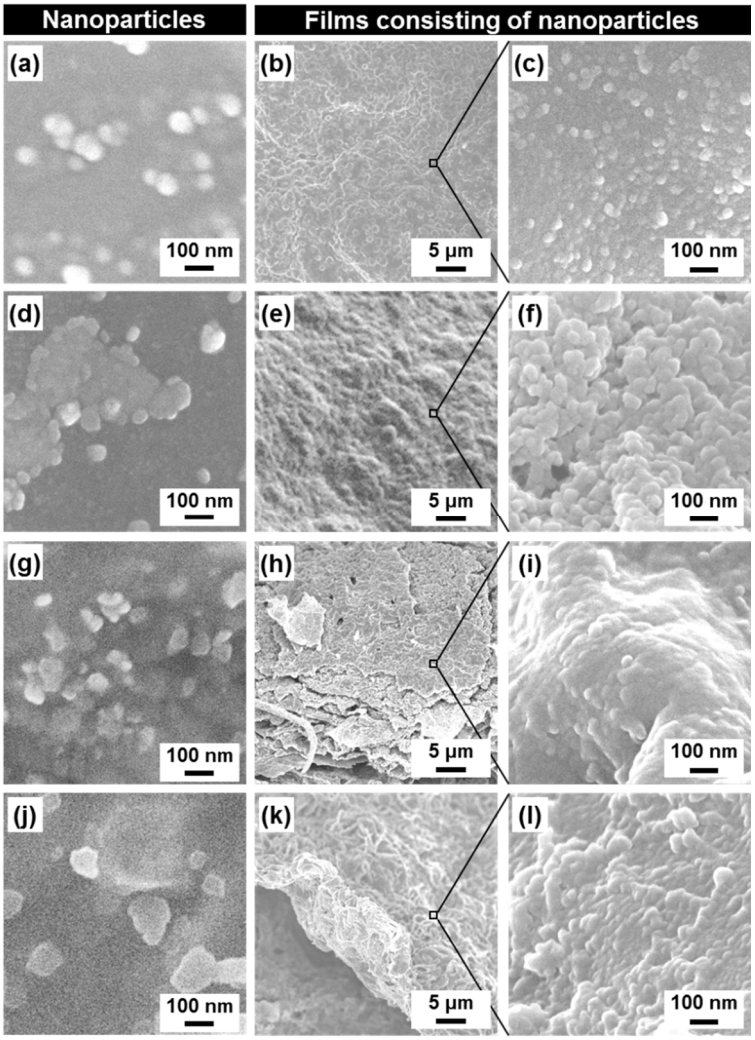

Fig. S4. FESEM images of the resultant PPy for 0.5 h (a) and 40 h (b,c), PEDOT for 3 h (d) and 64 h (e,f), PTp for 4 h (g) and 88 h (h,i), and P3HT for 5 h (j) and 112 h (k,l) on the surface of $FeCl_3$ crystals.

In PPy, PEDOT, PTp, and P3HT, the similar nanoparticles and their accumulated films were obtained. The morphology variations were similar to those of PANI on $Cu(NO_3)_2 \cdot 3H_2O$ crystals in Fig. 2.

FESEM images of the PPy reference samples

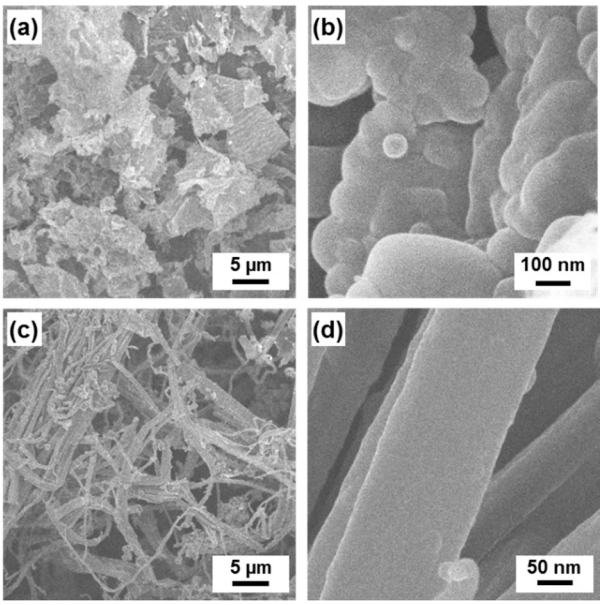

Fig. S5. FESEM images of the PPy films formed on the flat $CuSO_4 \cdot 5H_2O$ crystals (a,b) and commercial PPy fibrils (c,d).

The PPy films consisting of the nanoparticles around 100 nm in size were obtained after 38 h on the flat surface of $CuSO_4 \cdot 5H_2O$ crystals (Fig. S5a,b). A commercial PPy showed the microfibers 700 nm in width and up to 100 μm in length (Fig. S5c,d).

Electrochemical properties

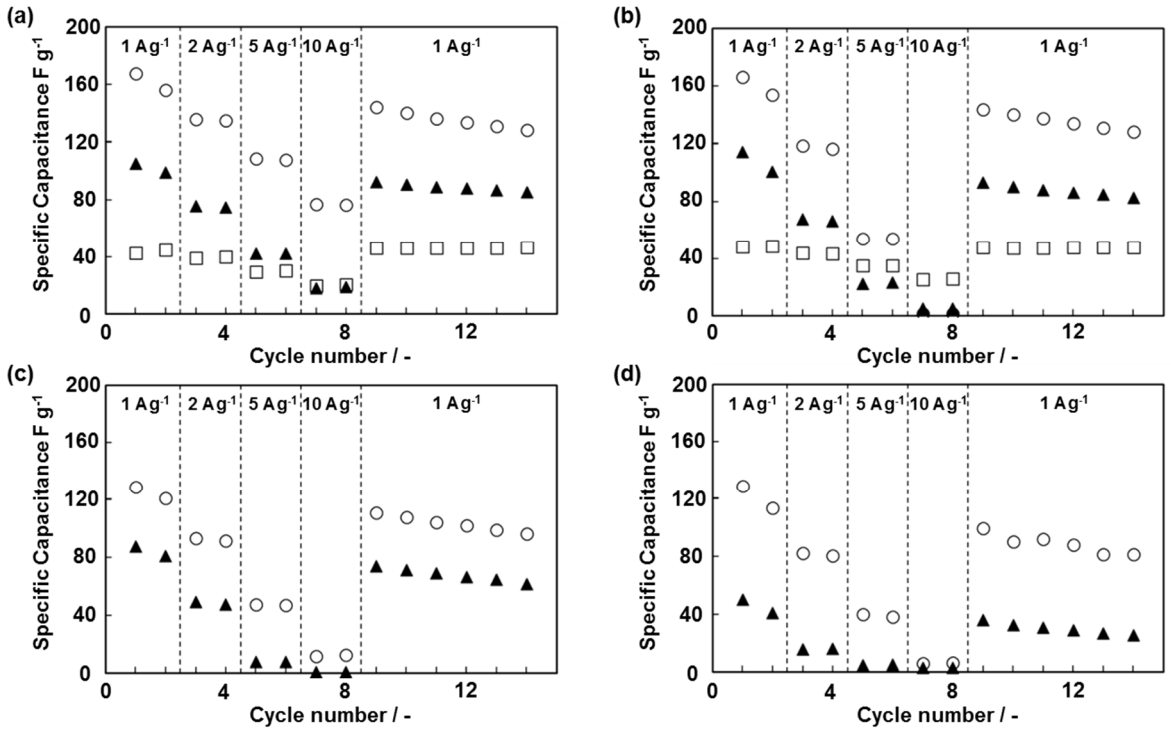

Fig. S6. Relationship between the current density and specific capacitance of PPy sponge with the hierarchical structures (circles), films consisting of the nanoparticles (triangles), and commercial fibers (squares). The electrochemical properties were measured on a number of samples prepared in the different batches and times (a–d). In the commercial fiber samples, the electrodes were prepared two different times (a,b). The panel (a) was the same as displayed in Fig. 3f.

In all the experiments, the highest specific capacitance was obtained on the resultant PPy sponge with the hierarchical structure rather than the other two reference samples. At the low current density, namely 1 A g^{-1} and 2 A g^{-1}, the values of specific capacity were almost consistent with these four samples. However, the specific capacity at the high current density, namely 5 A g^{-1} and 10 A g^{-1}, was not constant. It is inferred that the electron pass from the current collector to the PPy was not always formed in the working electrode. Since the resultant PPy sample was flocculate objects, the same homogeneous mixture of the PPy, carbon, and PVDF was not always prepared by the present manual method. Therefore, the electron pass from the current collector to the PPy was not always formed as the same states.